

Anisotropic diffusion of the state of polarization in optical fibers with randomly varying birefringence

P. K. A. Wai and C. R. Menyuk

Department of Electrical Engineering, University of Maryland, Baltimore County, Baltimore, Maryland 21228-5398

Received August 8, 1995

Polarization diffusion in communication fibers is studied. Diffusion of the states of polarization in an optical fiber is found to be anisotropic on the surface of the Poincaré sphere. The predicted anisotropy has significant implications for nonlinear evolution in long-distance communication systems. © 1995 Optical Society of America

Random fluctuations in birefringence along an optical fiber degrade the transmission rate in communication systems.¹ In modern, dispersion-shifted communication fibers, at typical data rates and transmission powers, the birefringent beat length is of the order of meters or tens of meters, whereas the dispersive and nonlinear scale lengths are typically hundreds of kilometers. Thus, although the index difference corresponding to the birefringence is small, $\Delta n \approx 10^{-7}$, the birefringence should be considered large, and its effect would be devastating except that the orientation of this birefringence is rapidly and randomly changing on a length scale of tens to hundreds of meters. Under these circumstances, if one assumes that the variation of the birefringence is so rapid that its only effect is to scramble the electric field on the Poincaré sphere, one finds that light propagation in both nonreturn-to-zero and soliton communication systems can be described by the Manakov equation.^{2–4} If one takes into account the finite fiber decorrelation length, one finds that additional terms that act as noise sources are added to the Manakov equation.^{2,4} These additional noise terms are both linear and nonlinear in field strength. The linear terms lead to the usual linear polarization mode dispersion, whereas the nonlinear terms will lead to a nonlinear polarization mode dispersion whose effects have barely begun to be explored.

In simulations of long-distance propagation in optical fibers, the practice has often been simply to scramble the electric field on the Poincaré sphere at fixed intervals while allowing the field to evolve deterministically in between. This approach tacitly assumes that the electric field diffuses uniformly on the Poincaré sphere. However, communication fibers are nearly linearly birefringent so that the polarization eigenaxes, even though randomly varying, are confined to the equator of the Poincaré sphere, and one might anticipate that the equatorial diffusion rate on the Poincaré sphere is not the same as the azimuthal diffusion rate. In this Letter we show that the electric-field diffusion on the Poincaré sphere is indeed anisotropic. This anisotropy affects the relative contribution of the linear and the nonlinear noise terms and thus has important implications for nonlinear pulse evolution.

In this Letter we use two different physical models^{4–6} to study the rate of diffusion of an input state of polariza-

tion on the Poincaré sphere as a function of fiber autocorrelation length h_{fiber} and beat length L_B . We may measure the diffusion lengths by calculating the variances of the Stokes parameters S_1 , S_2 , and S_3 and determining the lengths d_1 , d_2 , and d_3 at which the variances are within $1/e$ of the final asymptotic value of $1/3$. The diffusion lengths d_1 and d_2 correspond to equatorial diffusion along the Poincaré sphere. Both these lengths and the polarization decorrelation length h_E are physically related to the length over which the electric field loses memory of its orientation. By contrast, d_3 corresponds to azimuthal diffusion along the Poincaré sphere and is physically related to the length over which the electric field loses memory of the ratio between the minor and major axes of the polarization ellipse.

After we remove variation common to both polarizations components, the spatial dependence of the electric field $\mathbf{U}(r, \omega, z)$ is given by

$$\frac{\partial \mathbf{U}(r, \omega, z)}{\partial z} = i \begin{bmatrix} x & y \\ y & -x \end{bmatrix} \mathbf{U}(r, \omega, z), \quad (1)$$

where $(x^2 + y^2)^{1/2}$ is the birefringence. The beat length is given by $L_B = 2\pi/(x^2 + y^2)^{1/2}$. The coupling constant y is taken to be real because the fiber is assumed to be linearly birefringent, as is nearly the case for real communication fibers.

In the first model we assume the strength of the birefringence to be fixed but we allow the orientation to vary randomly, i.e., $x(\omega, z) = b(\omega) \cos \theta(z)$ and $y(\omega, z) = b(\omega) \sin \theta(z)$, where $b(\omega)$ does not depend on the distance z . We further assume that the rate of change of the angle θ of the orientation axes is a white-noise process, i.e., $d\theta/dz = g_\theta(z)$, $\langle g_\theta(z) \rangle = 0$, and $\langle g_\theta(z) g_\theta(z+u) \rangle = \Gamma \delta(u)$, where Γ is a constant and $\delta(u)$ is the Dirac delta function. The fiber autocorrelation length h_{fiber} is $2/\Gamma$. In the second model, both x and y vary independently according to the following Langevin equations: $dx/dz = -\alpha x + g_x(\omega, z)$ and $dy/dz = -\alpha y + g_y(\omega, z)$, where α is a constant and both $g_x(\omega, z)$ and $g_y(\omega, z)$ are white-noise processes with zero mean and the same distribution. The fiber autocorrelation length h_{fiber} is $1/\alpha$.

We now switch to the Poincaré representation of the field. Instead of following the evolution of the complex

fields $U_1(z)$ and $U_2(z)$, we will follow the evolution of the three real Stokes parameters $S_1 = U_1 U_1^* - U_2 U_2^*$, $S_2 = U_1 U_2^* + U_2 U_1^*$, and $S_3 = -i(U_1 U_2^* - U_2 U_1^*)$, where $U_1 = \mathbf{U} \cdot \hat{\mathbf{e}}_1(z)$ and $U_2 = \mathbf{U} \cdot \hat{\mathbf{e}}_2(z)$. We assume that the field \mathbf{U} is normalized so that $S_1^2 + S_2^2 + S_3^2 = 1$. There are two physically sensible choices of the orthogonal unit vectors $\hat{\mathbf{e}}_1(z)$ and $\hat{\mathbf{e}}_2(z)$. We may choose that they equal $\hat{\mathbf{e}}_1(z_0)$ and $\hat{\mathbf{e}}_2(z_0)$, the polarization eigenstates at the beginning of our simulations, or we may choose that they equal the local polarization eigenstates.

To study the anisotropy, we start our simulations on the equator of the Poincaré sphere by setting $(S_1, S_2, S_3)(z_0) = (1, 0, 0)$. We have repeated our simulations with $(S_1, S_2, S_3)(z_0) = (0, 1, 0)$, and we find that the results are qualitatively the same. We then repeatedly integrate Eq. (1) 1000 times with a fixed set of parameters, using different, randomly generated inputs for $g_\theta(z)$ in our first model or for $g_x(z)$ and $g_y(z)$ in our second model. These 1000 time histories constitute our ensemble that we then use to calculate the variances of S_i , which are the statistical quantities of interest. At large distances the polarization states of the electric field become uniformly distributed on the Poincaré sphere so that $\langle S_i \rangle \rightarrow 0$ and $\langle S_i^2 \rangle \rightarrow 1/3$. We define the diffusion length d_i as the distance at which the variance of S_i , $\sigma_i^2 = \langle S_i^2 \rangle - \langle S_i \rangle^2$ rises to $1/e$ of its asymptotic value $1/3$, where $i = 1, 2, 3$. Quantities that are measured with respect to local polarization eigenaxes are designated by the subscript local, and quantities that are measured with respect to the initial polarization eigenaxes are designated by the subscript fixed. We start in a pure state so that $\langle \sigma_i^2(z_0) \rangle = 0$.

In Fig. 1 we plot σ_i^2 versus distance, setting $h_{\text{fiber}} = 0.1L_B$ in the first model, in which the birefringence strength is fixed. The long-dashed curve gives $\sigma_{1,\text{local}}^2$, the short-dashed curve gives $\sigma_{2,\text{local}}^2$, the dotted curves give $\sigma_{1,\text{fixed}}^2$, and the dashed-dotted curve gives $\sigma_{2,\text{fixed}}^2$. The solid curve is the measurement of σ_3^2 . We note that the choice of reference axes does not affect S_3 , so that σ_3^2 is the same when measured with respect to both sets of axes. From Fig. 1 it is apparent that the diffusion lengths for the different Stokes parameters are different. We find that in a fiber fluctuation length both $\sigma_{1,\text{local}}^2$ and $\sigma_{2,\text{local}}^2$ increase from zero toward $1/2$, the expected variance if there is no azimuthal diffusion. Then both $\sigma_{1,\text{local}}^2$ and $\sigma_{2,\text{local}}^2$ approach $1/3$ on the same length scale at which σ_3^2 approaches $1/3$. When measured with respect to the initial eigenaxes, $\sigma_{1,\text{fixed}}^2$ and $\sigma_{2,\text{fixed}}^2$ steadily increase toward $1/3$ on a length scale longer than the length scale at which σ_3^2 approaches $1/3$. In other words, the equatorial diffusion length measured with respect to the local eigenaxes is shorter than the azimuthal diffusion length, which in turn is shorter than the equatorial diffusion length measured with respect to the fixed eigenaxes. From a physical standpoint, the electric field cannot follow the rapid changes in the axes of birefringence when $h_{\text{fiber}} \ll L_B$, and its orientation changes slowly. Thus with respect to the local eigenaxes the electric field will change rapidly, on the length scale h_{fiber} , whereas with respect to the

fixed eigenaxes it will change slowly, on a length scale L_B^2/h_{fiber} .⁶

The same ordering of the diffusion lengths does not hold when the fiber autocorrelation length is comparable with or longer than the beat length. In Fig. 2, we plot σ_i^2 versus distance for $h_{\text{fiber}} = 10L_B$ in the first model in which the birefringence strength is fixed. The curve types have the same meaning as in Fig. 1. The diffusion length $d_{1,\text{local}}$ for $\sigma_{1,\text{local}}^2$ is now the longest. The variance $\sigma_{2,\text{local}}^2$ and σ_3^2 are almost identical, whereas $\sigma_{1,\text{fixed}}^2$ and $\sigma_{2,\text{fixed}}^2$ have small oscillations with a period equal to the beat length. Although these small oscillations appear as sharp steps in Fig. 2, these are adequately resolved numerically because we use 500 points per the shorter of h_{fiber} and L_B in our simulations.

In Fig. 3 we plot the diffusion lengths d_i versus h_{fiber}/L_B for the first model, in which the birefringence strength is fixed. When measured with respect to the local eigenaxes, the diffusion lengths $d_{1,\text{local}}$ and $d_{2,\text{local}}$ are proportional to h_{fiber} , and $d_{1,\text{local}}$ is larger than $d_{2,\text{local}}$. With respect to the fixed eigenaxes, we find that the $d_{i,\text{fixed}}$ are proportional to $1/h_{\text{fiber}}$ when $h_{\text{fiber}} \ll L_B$ and proportional to h_{fiber} when $h_{\text{fiber}} \gg L_B$. When $h_{\text{fiber}} \ll L_B$ we find that $d_{2,\text{local}} \approx d_3$ and when $h_{\text{fiber}} \gg L_B$ we find that $d_{1,\text{fixed}} \approx d_{2,\text{fixed}} > d_3$. In Fig. 4 we plot the diffusion lengths of

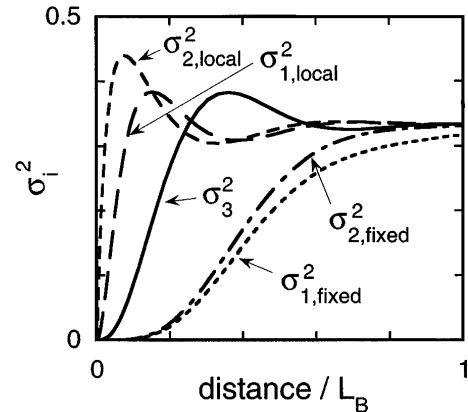


Fig. 1. Variances of the Stokes parameters. The σ_i^2 are plotted versus distance for $h_{\text{fiber}} = 0.1L_B$ in the first model, in which the strength of birefringence is fixed but the orientation varies randomly.

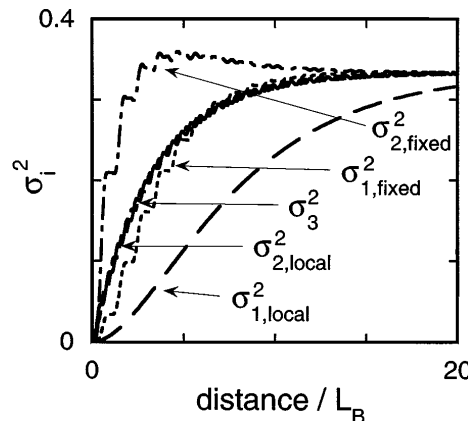


Fig. 2. Variances of the Stokes parameters. The σ_i^2 are plotted versus distance for $h_{\text{fiber}} = 10L_B$ in the first model.

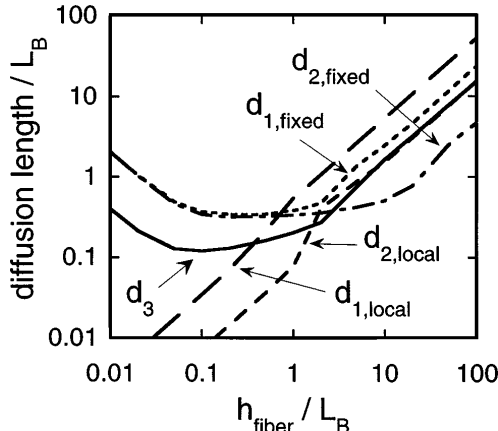


Fig. 3. Diffusions length d_i versus h_{fiber}/L_B for the first model.

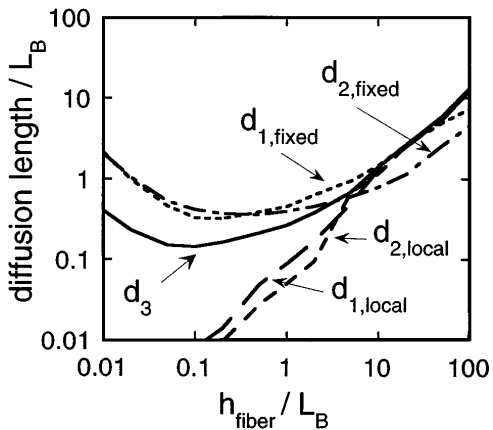


Fig. 4. Diffusion lengths d_i versus h_{fiber}/L_B for the second model, in which both the strength and the orientation of the birefringence vary randomly.

σ_i^2 versus h_{fiber}/L_B for the second model, in which both the birefringence strength and orientation vary. The results are qualitatively similar to those of the first model, shown in Fig. 3, so that including the variation of the strength of the birefringence does not have a significant effect on the diffusion lengths d_i .

As a simple example of how the anisotropic field diffusion on the Poincaré sphere can affect the nonlinear evolution, we consider the case in which the initial input to the optical fiber is in a single state of polarization, $\hat{\mathbf{e}}_1(z_0)$, as a function of time. At low intensities the polarization state of the central frequency will undergo a complex evolution through a sequence of states $\hat{\mathbf{e}}_1(z)$. Different frequencies will undergo a somewhat different evolution, and the Kerr effect will also lead to a somewhat different evolution. Referring to the complex amplitude in the polarization state $\hat{\mathbf{e}}_1(z)$ as $U(z, t)$ and the complex amplitude in the orthogonal polarization state as $V(z, t)$, we have shown that the evolution of $U(z, t)$ and $V(z, t)$ is governed by the Manakov equation with additional noise terms.^{2,4} If

we set $(U, V)(z_0) = (U_0, 0)$ and the nonlinear and chromatic dispersive scale lengths are long compared with the scale lengths for linear and nonlinear polarization mode dispersion, then

$$\begin{aligned} V(z, t) = & -b' \left(\int_0^z dz' c_1 \right) \frac{\partial U_0}{\partial t} \\ & + i \frac{1}{3} \left(\int_0^z dz' c_2 \right) |U_0|^2 U_0, \end{aligned} \quad (2)$$

where c_1 and c_2 are complex coefficients. For the first model, with constant birefringence, the evolutions of c_1 and c_2 are given by that of S_1 with respect to the local axes and S_3^2 , respectively, with the appropriate initial conditions.⁴ The relative contribution of the linear and the nonlinear noise terms depends on the ratio of the equatorial diffusion length to the azimuthal diffusion length.

In conclusion, using two physically reasonable models, we show that the diffusion length of the Stokes parameters is a function of both h_{fiber} and L_B . We have demonstrated that the diffusion is anisotropic in general. This anisotropy can have important consequences for the nonlinear evolution of light in optical fibers and for current practice in simulations that randomizes the electric field on the Poincaré sphere at a fixed interval.

This work was supported by the National Science Foundation and the U.S. Department of Energy. Computational work was carried out at the National Energy Research Supercomputer Center and the San Diego Supercomputing Center.

References

1. C. D. Poole and R. E. Wagner, Electron. Lett. **22**, 1029 (1986); C. D. Poole, Opt. Lett. **13**, 687 (1988); **14**, 523 (1989); C. D. Poole, J. H. Winters, and J. A. Nagel, Opt. Lett. **16**, 372 (1991); G. J. Foschini and C. D. Poole, J. Lightwave Technol. **9**, 1439 (1991).
2. P. K. A. Wai, C. R. Menyuk, and H. H. Chen, Opt. Lett. **16**, 1231 (1991).
3. S. G. Evangelides, Jr., L. F. Mollenauer, J. P. Gordon, and N. S. Bergano, J. Lightwave Technol. **10**, 28 (1992).
4. P. K. A. Wai and C. R. Menyuk, submitted to J. Lightwave Technol.
5. C. R. Menyuk and P. K. A. Wai, J. Opt. Soc. Am. B **11**, 1288 (1994). In this paper it is stated that the theoretical approach applies to a lossless fiber. The approach applies equally well to a fiber with polarization-independent loss, since we need merely allow k_0 to be complex in Eq. (5), and the transformation that removes k_0 in Eq. (6) still works. However, the theoretical approach does not apply to a fiber with polarization-dependent loss, and a modified approach is needed.
6. P. K. A. Wai and C. R. Menyuk, Opt. Lett. **19**, 1517 (1994).